Remote Sensing of Environment 258 (2021) 112401

Contents lists available at ScienceDirect

Remote Sensing of Environment

journal homepage: www.elsevier.com/locate/rse

Evaluating plant photosynthetic traits via absorption coefficient in the photosynthetically active radiation region

Anatoly Gitelson [a,b,*], Timothy Arkebauer [c], Andrés Viña [d,e], Sergii Skakun [f], Yoshio Inoue [g]

[a] School of Natural Resources, University of Nebraska-Lincoln, Lincoln, NE 68583, USA
[b] Israel Institute of Technology (Technion), Haifa 3200003, Israel
[c] Department of Agronomy and Horticulture, University of Nebraska-Lincoln, Lincoln, NE 68583, USA
[d] Center for Systems Integration and Sustainability, Department of Fisheries and Wildlife, Michigan State University, Lansing, MI 48823, USA
[e] Geography Department, University of North Carolina, Chapel Hill, NC 27599, USA
[f] Department of Geographical Sciences, University of Maryland, 1153 LeFrak Hall, College Park, MD 20742, USA
[g] Graduate School of Engineering, The University of Tokyo, Tokyo 113-8656, Japan

ARTICLE INFO

Editor: Jing M. Chen

Keywords:
Absorption coefficient
Chlorophyll
Photosynthetically active radiation
PAR region

ABSTRACT

Absorption of radiation in the photosynthetically active radiation (PAR) region is significantly influenced by plant biochemistry, structural properties, and photosynthetic pathway. To understand and quantify the effects of these traits on absorbed PAR it is necessary to develop practical and reliable tools that are sensitive to these traits. Using a semi-analytical modeling framework for deriving the absorption coefficient of plant canopies from reflectance spectra, we quantify the effects of functional, structural and biochemical traits of vegetation on the relationship between the absorption coefficient in the PAR region (α_{par}) with canopy characteristics such as the fraction of PAR absorbed by photosynthetically active vegetation ($fAPAR_{green}$) and chlorophyll (Chl) content. The reflectance dataset used in the study included simulated data obtained from a canopy reflectance model (PROSAIL) and empirical data on three diverse crop species with different leaf structures, canopy architectures and photosynthetic pathways (rice, maize and soybean) acquired at proximal (i.e., using field spectroradiometers) and remote (i.e., Landsat TM and ETM+) distances. Results show the usefulness of α_{par} derived from reflectance data for assessing not only the photosynthetic status of vegetation, but also the effects of different functional, structural and biochemical traits on plant performance. Furthermore, these assessments can be made using data acquired by satellite sensor systems such as the Landsat series, which are available since the 1980s, thus facilitating the analysis of the photosynthetic status of terrestrial ecosystems throughout the world with a high temporal depth.

1. Introduction

While it is evident that all plant species are well adapted to their particular environments, the specific anatomical and physiological characteristics required for such adaptation are not equally evident. Of special interest are the effects of different photosynthetic pathways, which are associated not only with differences in plant biochemistry, but also with anatomical and structural differences at both leaf and canopy scales. For instance, C3 and C4 plant species, as well as monocots and dicots, exhibit different cell arrangements and chloroplast distributions within their leaves resulting in significant differences in the capacity of plant species to absorb photosynthetically active radiation (PAR), convert carbon dioxide and water into sugars through photosynthesis, and ultimately survive in different environments characterized, among many other things, by contrasting radiation levels (Gitelson et al., 2018; Langdale, 2011; Sage and Sultmanis, 2016; Young et al., 2020).

To understand the different effects of these traits on the absorption of radiation in the PAR region, it is necessary to develop tools that are not only sensitive to these effects but that are also practical and reliable. A semi-analytical modeling framework for deriving the absorption coefficient of plant canopies from canopy reflectance spectra was recently developed in the form $\alpha_\lambda = (\rho_{NIR}/\rho_\lambda) - 1$ (Gitelson et al., 2019), where ρ_{NIR} is reflectance in the near-infrared (NIR) region, while ρ_λ is reflectance at wavelength λ in the visible and red edge regions. This model is based on the partitioning of the total absorption coefficient into its photosynthetic and non-photosynthetic pigment components, while also

* Corresponding author at: School of Natural Resources, University of Nebraska-Lincoln, Lincoln, NE 68583, USA.
E-mail address: agitelson2@unl.edu (A. Gitelson).

https://doi.org/10.1016/j.rse.2021.112401
Received 22 September 2020; Received in revised form 8 March 2021; Accepted 13 March 2021

Table 1
Summary of experimental data sets.

Crops	Year	# of Plots	Sensor, spectral range, nm	Distance, FOV	Leaf [Chl]	LAI	Plant type
Rice (*Oryza sativa* L. *japonica* variety)	2009	64	ASD 350–2500	2 m, 25^{O}	Chemical	Destructive	Erectophile, narrow leaves
Maize (*Zea mays* L.)	2003–2005	118	USB2000 400–900	5.5 m, 25^{O}	Non-destructive and Chemical	Destructive	Plagiophile, long broad leaves
Soybean (*Glycine max* (L.) Merr.)	2002, 2004	73	USB2000 400–900	5.5 m, 25^{O}	Non-destructive and Chemical	Destructive	Planophile, round leaves

accounting for leaf and canopy backscattering. The model allows derivation of the absorption coefficient spectra throughout the PAR and the red-edge spectral regions while also facilitating an accurate estimation of canopy chlorophyll content (Gitelson et al., 2019). As such, the model brings not only important information about the physiological and phenological status of plants, but also about their photosynthetic potential. But in addition to its sensitivity to these characteristics, the model is also sensitive to both structural and biochemical traits, making it potentially suitable for assessing the effects of these different traits on light absorption and ultimately on photosynthesis rates and chlorophyll efficiency [i.e., primary production per chlorophyll content (Gitelson et al., 2016)] across different plant species.

Based on these premises, we hypothesize that the absorption coefficient in the PAR region is not only closely related with the fraction of PAR absorbed by the photosynthetic component of plant canopies ($fAPAR_{green}$) and with canopy Chl, but also that these relationships are influenced by structural (e.g., leaf structure, canopy architecture) and biochemical (e.g., photosynthetic pathways) plant traits. Therefore, the absorption coefficient derived from reflectance spectra may be used as a suitable remotely derived proxy of these structural and functional vegetation traits. The study evaluates the relationships between the reflectance-based absorption coefficient in the PAR spectral region (α_{par}) with $fAPAR_{green}$, with leaf chlorophyll content [Chl], and with canopy [Chl] (the product of leaf [Chl] and leaf area index, LAI). To assess the effects of these different plant traits on α_{par}, the relationships were evaluated in three contrasting crop species (maize – *Zea mays* L.; soybean – *Glycine* max (L.) Merr.; rice – *Oryza sativa* L.) having different leaf structures, canopy architectures and photosynthetic pathways. The relationships were evaluated at canopy and field scales using reflectance data acquired at close range through hyperspectral sensors, and through multispectral sensors onboard Earth observation satellites (i.e., Landsat series), respectively. The latter facilitates both the study of these relationships across the globe, as well as the assessment of their temporal dynamics as these satellite data have been available since the 1980s.

2. Materials and methods

The study used multiple datasets of the three crop species evaluated (i.e., maize, soybean and rice) acquired for different studies (Ciganda et al., 2009; Gitelson et al., 2019; Gitelson et al., 2018; Gitelson and Gamon, 2015; Gitelson et al., 2016; Gitelson et al., 2005; Gitelson et al., 2008; Gitelson et al., 2006; Inoue et al., 2016; Nguy-Robertson et al., 2012; Peng et al., 2011; Peng et al., 2017; Viña and Gitelson, 2005; Viña et al., 2011) in separate sites, across different years and at scales ranging from individual leaves to entire fields. While there is some variation among datasets since the studies were performed across multiple scales, at different times, and in different places, the data collection techniques employed constitute standard procedures. The following paragraphs summarize the procedures employed. For more details on the different data collection procedures, the reader should consult the cited papers.

2.1. Study sites

Maize and soybean data collection campaigns were carried out during the growing seasons (from May to September) of 2001 to 2008 in three AmeriFlux sites (US-Ne1, US-Ne1, and US-Ne3), located near Mead, Nebraska, USA. Both equipped with a center-pivot irrigation system, site 1 was under maize continuously, while site 2 was under a maize-soybean rotation (with maize in odd and soybean in even years). Site 3 was also under a maize-soybean rotation but relied entirely on rainfall (Verma et al., 2005). Rice data collection campaigns were carried out during the growing season of 2009 in ten experimental plots in Tsukuba, Japan. To induce a wide range of canopy responses, four different nitrogen levels (2, 6, 14, and 16 g m^{-2}) were applied (Inoue et al., 2016).

2.2. Reflectance at Canopy scale (i.e., close range)

In maize and soybean fields, canopy reflectance was measured using two inter-calibrated Ocean Optics USB2000 radiometers (Table 1). One radiometer was equipped with a 25° field-of-view optical fiber pointing downward to measure canopy upwelling radiance within a 2.4 m^2 sampling area by placing the fiber at a height of approximately 5.5 m above the top of the canopy. The other sensor was equipped with an optical fiber and a cosine diffuser pointing upward to measure downwelling irradiance. Percent canopy reflectance was calculated as the ratio of upwelling radiance to downwelling irradiance (Rundquist et al., 2004; Viña et al., 2011). Canopy reflectance for each date was calculated as the median value of 36 reflectance measurements collected along access roads into each of the fields. In the rice fields, reflectance measurements were taken using a portable FieldSpec-Pro ASD spectroradiometer with a 25° field-of-view at a nadir-looking angle from 2 m above the canopy (Table 1). Percent canopy reflectance was calculated as the ratio of this upwelling radiance to that of a Spectralon-Labsphere white reference (Inoue et al., 2016). More than 30 spectra were averaged for each plot to derive the representative reflectance spectra. Absorption coefficient in the PAR spectral region was then calculated as:

$$\alpha_{par} = \left[\rho_{NIR}/\rho_{par}\right] - 1 \quad (1)$$

where ρ_{NIR} is the average of reflectance values in the NIR spectral region (750–900 nm), and ρ_{par} is the average of reflectance values in the PAR spectral region (400–700 nm).

2.3. Green leaf area index (LAI)

Green LAI of maize and soybean canopies was determined destructively from samples collected in six small plots (20 m × 20 m) established within each sampling site, representing major soil and crop production zones within each site (Verma et al., 2005). In the laboratory, green leaf samples were run through a LI-3100, Li-Cor area meter to calculate leaf area per plant. This area was then multiplied by the plant population (assessed in each plot) to obtain green LAI for each of the six plots, which were then averaged to obtain a site-level green LAI value (Viña et al., 2011). In the rice fields, five hills per plot were sampled randomly for destructive measurements and analysis in the lab. Green LAI was determined using an LI-3100C, Li-Cor area meter after carefully removing all senescent leaf parts (Inoue et al., 2016).

Table 2
Parameters in the PROSAIL model used to generate spectra for maize, rice and soybean. Viewing geometry was as follows: solar zenith angle was 30°, and observer zenith angle and azimuth angles were 0°. LAD is the leaf angle distribution; N is the leaf structure parameter; Cab is the leaf chlorophyll content; Car is the carotenoid content; Cbr is the brown pigment fraction; Cw is the water content; Cm is the dry matter content; and LAI is the leaf-area index.

Crop	LAD	N	Cab, μg cm^{-2}	Car, μg cm^{-2}	Cbr	Cw, cm	Cm, g cm^{-2}	LAI
Maize	Plagiophile	1.4–1.8	40–70	8–20	0–0.1	0.01–0.03	0.001	0.2–6.0
Soybean	Planophile	1.1–1.5	35–70	8–20	0–0.1	0.001–0.03	0.00075	0.2–5.6
Rice	Erectophile	1–2	20–40	5–10	0–0.1	0.001–0.03	0.0005–0.0015	0.2–6.5

2.4. Chlorophyll content

The Chl content ([Chl]) of leaves sampled in maize and soybean fields (ear leaf in maize plants and the top-most fully expanded leaf in soybean plants) was measured destructively in the lab, concurrently with spectral reflectance measurements of the same leaves using an Ocean Optics radiometer equipped with a leaf clip. Foliar reflectance measurements were used to calculate the red edge chlorophyll index [$CI_{red\ edge} = (\rho_{NIR}/\rho_{720–730})$ -1], where ρ_{NIR} is reflectance in the NIR range 780–800 nm and $\rho_{720–730}$ is reflectance in the range between 720 and 730 nm. $CI_{red\ edge}$ was linearly related with the destructive lab measurements of leaf [Chl]. The relationship [Chl] vs. $CI_{red\ edge}$, calibrated on a per-year basis, was then used to retrieve leaf [Chl], which multiplied by LAI provides an estimate of canopy [Chl] (Ciganda et al., 2009; Gitelson et al., 2005; Gitelson et al., 2006). In rice, five hills per plot were randomly sampled for obtaining a measure of leaf [Chl] using a chemical analysis in the laboratory. Canopy [Chl] was then obtained by multiplying leaf [Chl] by the biomass of green leaves per m^2 of ground area (Inoue et al., 2016).

2.5. Fraction of absorbed photosynthetically active radiation (fAPAR) by crop canopies

In maize and soybean fields, measurements of incoming PAR (PARinc) were obtained using Li-Cor point quantum sensors placed at 6 m above the ground pointing to the sky, while measurements of PAR reflected by the canopy and the soil background (PARout) were obtained using Li-Cor point quantum sensors also placed at 6 m from the ground pointing downward. PAR transmitted through the canopy (PARtransm) was measured using five Li-Cor line quantum sensors placed diagonally across the crop rows, approximately 1 m apart and at about 2 cm above the ground looking upward. PAR reflected by the soil (PARsoil) was measured with Li-Cor line quantum sensors placed about 12 cm above the ground, looking downward (Viña and Gitelson, 2005). PAR absorbed by the crop canopy (APAR) was calculated as APAR = PARinc–PARout – PARtransm + PARsoil (Goward and Huemmrich, 1992), while the fraction of APAR absorbed by the crop canopy (*f*APAR) was obtained as $fAPAR = APAR/PAR_{inc}$. The green component of *f*APAR (i.e., absorbed only by the photosynthetically active component of the canopy; $fAPAR_{green}$), was obtained as $fAPAR_{green} = fAPAR*(LAI_{green}/LAI_{total})$ (Viña and Gitelson, 2005).

2.6. Reflectance at field scale (i.e., Landsat imagery)

To maximize the number of cloud-free images acquired during the field sampling period, imagery at 30-m spatial resolution from both Landsat-5 Thematic Mapper (TM) and Landsat-7 Enhanced Thematic Mapper Plus (ETM+) were used (Wulder et al., 2019). The digital numbers of these images were converted to top-of-atmosphere (TOA) reflectance, and then atmospherically corrected to surface reflectance using the Landsat Ecosystem Disturbance Adaptive Processing System (LEDAPS) at NASA Goddard Space Flight Center (GSFC) (Masek et al., 2006). Reflectance values for the study sites were calculated by averaging all the per-pixel values within a field, and these Landsat-retrieved site spectral reflectance values were paired with corresponding canopy chlorophyll content measurements (Gitelson et al., 2008). Absorption coefficient in the PAR region was then calculated as.

$$\alpha_{par} = \{\rho_4/[(\rho_1 + \rho_2 + \rho_3)/3]\}–1 \quad (2)$$

where ρ_λ is surface reflectance values in Landsat TM/ETM+ spectral bands 4 (NIR: 760–900 nm), 1 (blue: 450–520 nm), 2 (green: 520–600 nm) and 3 (red: 630–690 nm), respectively.

2.7. Simulation of crop reflectance spectra

The leaf angle distribution (LAD) in the crops studied is highly contrasting, from the erectophile LAD of rice, to the planophile and plagiophile LADs of soybean and maize, respectively. To assess the effects of different LAD on canopy reflectance a radiative transfer PROSPECT + SAIL model combination, termed PROSAIL (Version 5B) (Féret et al., 2017; Jacquemoud et al., 2009) was used to model maize, rice and soybean reflectance spectra under different plant conditions. PROSAIL simulates canopy spectra based on foliar (chlorophyll, carotenoid and brown pigment contents, dry matter, water content, structure), soil (dry/wet) and canopy (LAI, LAD, hot spot, solar and observing angles) properties. Table 2 summarizes the input parameters used in the PROSAIL simulations. Two scenarios were simulated, named hereafter Case A and Case B. In Case A, input parameters were sampled from minimum to maximum values, as suggested in Inoue et al., (2016), without any constraints; while in Case B, LAI and leaf chlorophyll content were constrained to follow the relationships between LAI and canopy Chl content established empirically in this study for maize, rice and soybean (Table 3).

3. Results and discussion

3.1. Empirical analyses

Green LAI, leaf [Chl] and canopy [Chl] varied widely among the crops studied, with maize exhibiting the largest values (Table 3). For instance, the average leaf [Chl] of maize was almost twice as large as those of soybean and rice, while the average canopy [Chl] of maize was

Table 3
Minimum (Min), maximum (Max), average (Mn) and median (Md) leaf (in μg cm^{-2}) and canopy (in g m^{-2}) chlorophyll contents, and green leaf area index values (in m^2 m^{-2}) empirically obtained in the maize ($N = 124$), soybean ($N = 73$), and rice ($N = 64$) fields sampled.

	Maize				Soybean				Rice			
	Min	Max	Mn	Md	Min	Max	Mn	Md	Min	Max	Mn	Md
Leaf [Chl]	23.1	80.0	56.7	58.1	8.0	62.3	35.8	36.2	15.2	58.4	32.2	29.4
Canopy [Chl]	0.07	3.61	2.04	2.13	0.03	2.69	1.07	0.97	0.01	2.13	0.63	0.53
LAI_{green}	0.17	5.52	3.49	4.04	0.16	5.45	2.59	2.62	0.08	6.73	2.13	2.14

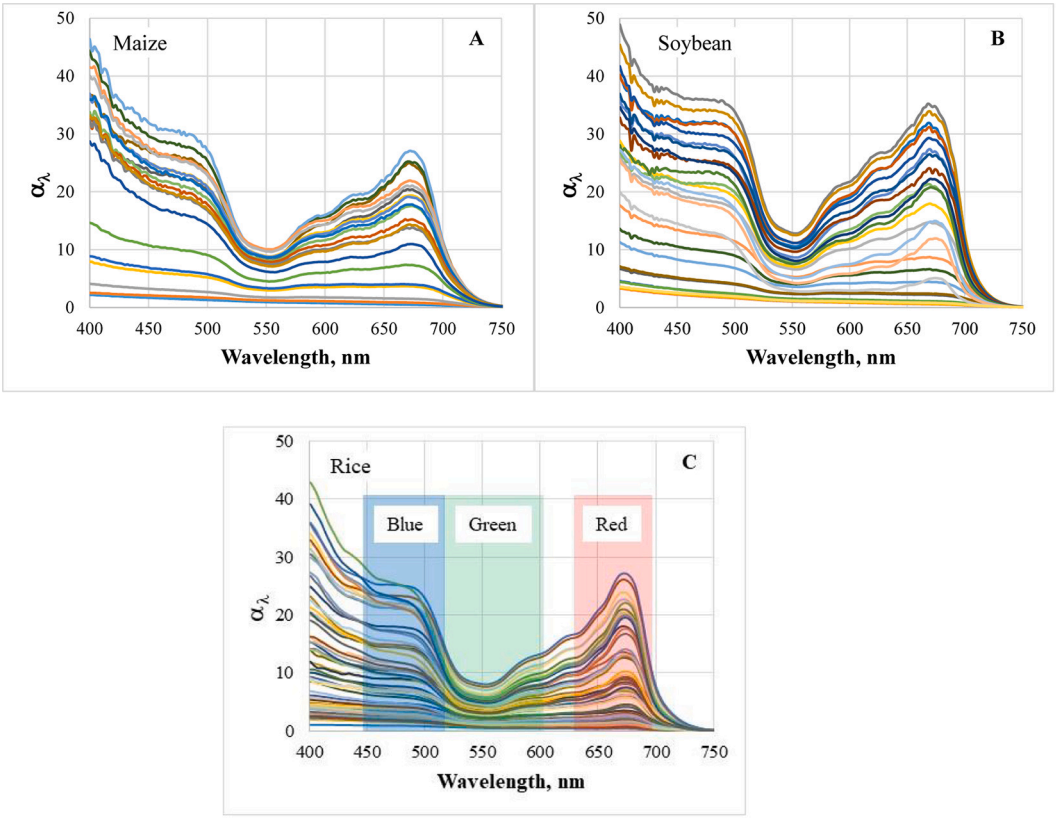

Fig. 1. Spectral absorption coefficient α_λ of maize (A), soybean (B), and rice (C) crops retrieved from canopy reflectance spectra acquired during the growing seasons. Spectral curves at the bottom of the figures correspond to soil/residue and late stage of senescence while those at the top were taken at the time of maximal leaf area index and chlorophyll content. In panel C spectral bands of Landsat TM and ETM+ in the PAR region are indicated.

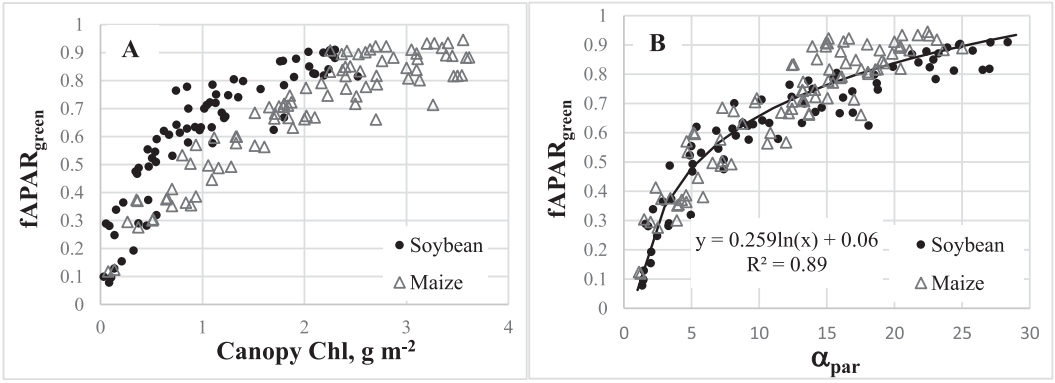

Fig. 2. Fraction of Photosynthetically Active Radiation (PAR) absorbed by the photosynthetically active (i.e., green) portion of maize and soybean canopies ($fAPAR_{green}$) vs. canopy [Chl] (A), and $fAPAR_{green}$ vs. absorption coefficient in the PAR region 400–700 nm (α_{par}) (B).

2-fold and 4-fold larger than those of soybean and rice, respectively (Table 3). Average green LAI of maize was not as large when compared to those of soybean and rice, but was still 25% and 38% larger, respectively (Table 3).

The α_λ spectra obtained from reflectance spectra of crop canopies exhibited two maximal values, one in the blue (400–500 nm) and another in the red (650–700 nm) spectral regions (Fig. 1). It is notable that the values of α_λ in the green (500–580 nm) spectral region reach 34% (in maize), 38% (in soybean) and 31% (in rice) of those in the red region. This constitutes a more than 3-fold larger value than the green/red or the green/blue ratios of leaf specific absorption coefficient of Chl (Féret et al., 2017). This also demonstrates a 20-fold larger absorption capability of the canopy as compared to absorption coefficient of Chl in vitro, where the absorption coefficient in the green region does not exceed 1–1.5% of the value in the red region (Lichtenthaler, 1983). Therefore, canopy α_λ exhibits an important source of variability that is not captured by α_λ in leaves or in vitro.

$fAPAR_{green}$, which is an important functional characteristic of crop canopies related with gross primary productivity and constitutes a key factor defining light use efficiency, exhibited a close non-linear relationship with canopy [Chl] in both maize and soybean (Fig. 2A). Furthermore, for the same magnitude of canopy [Chl], $fAPAR_{green}$ was significantly higher in soybean than in maize. Nevertheless, the relationships of $fAPAR_{green}$ vs. α_{par} for maize and soybean were quite similar despite their differences in leaf structure (i.e., monocot vs. dicot), canopy architecture (i.e., plagiophile vs. planophile leaf angle

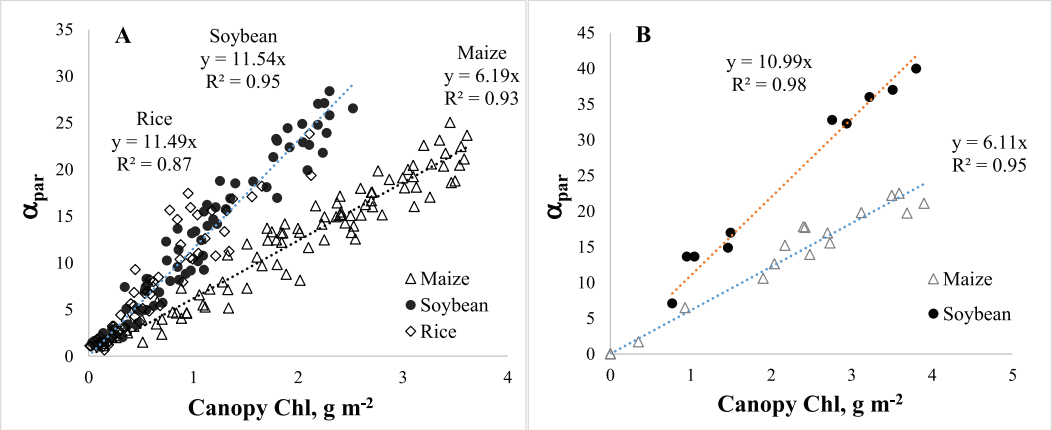

Fig. 3. Relationships between the absorption coefficient in the PAR region (α_{par}) and canopy [Chl] (A) at canopy scale (i.e., close range using hyperspectral radiometers) for maize, soybean, and rice, and (B) at field scale (i.e., Landsat pixel) for maize and soybean. Data shown were obtained across different growing seasons (i.e., 2002–2005 and 2009; see Table 1).

distribution) and photosynthetic pathway (i.e., C4 vs. C3) (Fig. 2B). At the beginning of the growing season, $fAPAR_{green}$ exhibited a sharp increase of up to 0.6–0.7 as LAI_{green} reached 2.5–3 m^2 m^{-2} in both maize and soybean, while later in the season, when the LAI_{green} and the α_{par} increased significantly (e.g., up to 2.5 to 3-fold increase was observed in α_{par}, corresponding to more than 60% of its entire dynamic range), $fAPAR_{green}$ changed from 0.7 to 0.95. Thus, the slope of the $fAPAR_{green}$ vs. α_{par} relationship at this stage decreased about 5-fold compared to that at the beginning of the growing season. This can be explained by a decrease in Chl efficiency with an increase in canopy density due to self-shadowing (Gitelson et al., 2016). Yet, even though Chl efficiency declines, α_{par} remained sensitive to the increase in $fAPAR_{green}$, therefore it may be used as a proxy of $fAPAR_{green}$ (Fig. 2B).

The relationships of α_{par} and canopy [Chl] were linear at both canopy scales, acquired at close-range (Fig. 3A), and field scales, retrieved from Landsat TM and ETM+ imagery (Fig. 3B). This means that the sensitivity of α_{par} to Chl content remains almost invariant over a wide range of chlorophyll contents that vary through time (i.e., among phenological states) from the beginning of the growing season to maximal canopy density, and into senescence. This is in contrast with the relationship between α_{par} and chlorophyll content at the leaf level, which is essentially non-linear due to the saturation of reflectance in the main absorption bands of chlorophyll (blue and red) at moderate-to-high leaf chlorophyll contents. The linear response of α_{par} to canopy chlorophyll content is due to the close relation between canopy chlorophyll and green leaf area index (Ciganda et al., 2008). The latter increases with an increase in canopy density and thus compensates the decrease in sensitivity to chlorophyll content of reflectance in the red and blue regions of the spectrum (Gitelson et al., 2019).

It is important to underline that while the slopes of the relationships were very similar for soybean and rice, the slope for maize was almost two-fold smaller at both canopy and field scales (Fig. 3). This means that for the same canopy [Chl], α_{par} in soybean and in rice was about two-fold higher than in maize. Therefore, these C3 crops seem to exhibit a significantly larger amount of absorbed radiation per unit of [Chl] than maize, a C4 crop, as was shown for $fAPAR_{green}$ (Fig. 2A).

The variability of canopy [Chl] is significantly influenced by the development of the crop canopy throughout the growing season. While during the vegetative stage the variability of crop canopy [Chl] is affected by leaf [Chl] (Houborg et al., 2015; Schull et al., 2015), for the most part it depends on LAI, as it increases from zero to its maximal values. During the vegetative stage there is little senescent tissue and, hence, the total LAI (green plus senescent) is very similar to the green LAI. In contrast, while total LAI remains almost invariant during the reproductive stage, the senescent fraction increases, particularly in maize; canopy [Chl] continues to vary but this time in response mainly to both changes in green LAI and in leaf [Chl]. These temporal patterns of leaf and canopy [Chl] were found to be similar in maize and soybean canopies (Figs. 4A & 4B). Thus, *in reproductive and senescent stages, the relationship between leaf [Chl] and canopy [Chl] were almost linear and indistinguishable between these crops* (Fig. 5A).

Based on these results and on the significant linear relationships found between canopy [Chl] and α_{par} in the crops studied at both canopy and field scales and throughout several growing seasons (Fig. 3), we were interested in evaluating whether leaf [Chl] also exhibits a significant relationship with α_{par}. Fig. 5B shows close linear leaf [Chl] vs. α_{par} relationships with quite different slopes for maize and soybean. This is an interesting result given the long time period within the growing

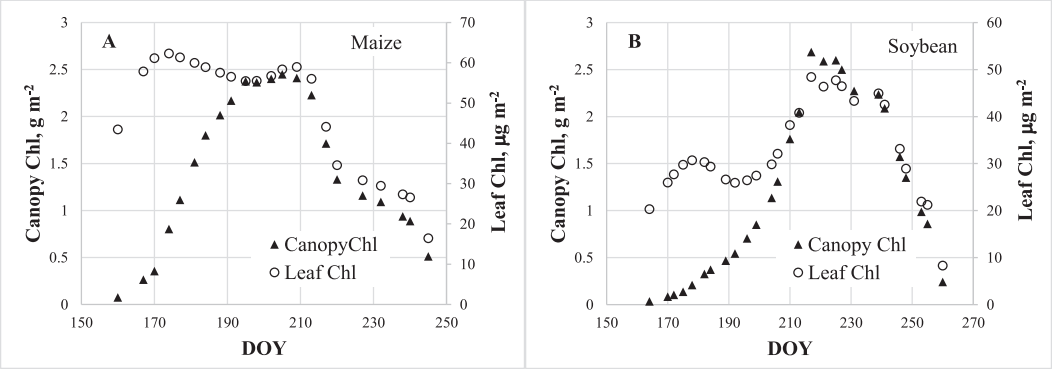

Fig. 4. Temporal progression of canopy [Chl] and leaf [Chl] throughout the growing season in (A) maize and (B) soybean. DOY is day of the year.

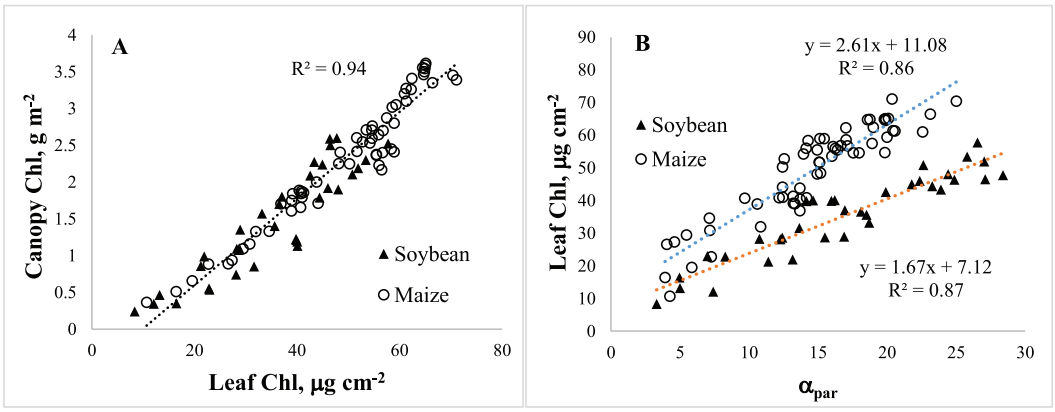

Fig. 5. Relationships of (A) canopy [Chl] vs. leaf [Chl] and (B) leaf [Chl] vs. canopy α_{par} in reproductive and senescent stages for maize and soybean.

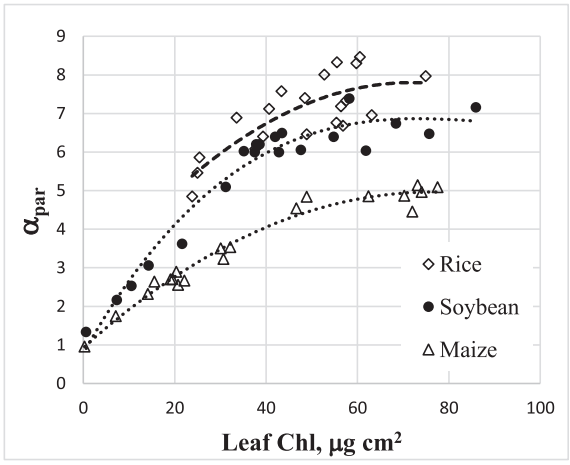

Fig. 6. Leaf absorption coefficient in the PAR region plotted versus leaf chlorophyll content in rice, maize, and soybean.

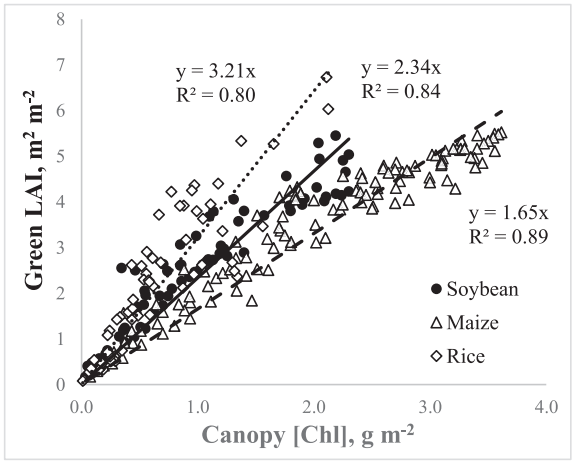

Fig. 7. Green LAI vs. canopy [Chl] in maize, soybean and rice. Canopy [Chl] = leaf [Chl] × green LAI. The slope of green LAI vs. canopy [Chl] relationship is (leaf [Chl])$^{-1}$.

season when *total* LAI is virtually invariant and canopy [Chl] is governed mainly by leaf [Chl]. Therefore, it lays a solid foundation for assessing leaf [Chl] content using α_{par} derived from canopy reflectance.

The canopy absorption coefficient in the PAR region was found to be sensitive to functional and structural traits such as $fAPAR_{green}$, canopy [Chl] and leaf [Chl] in quite contrasting crop species. These species not only allocate scarce resources, such as nitrogen, in different ways (Quebbeman and Ramirez, 2016) but also exhibit different structural and biochemical characteristics. All these differences drive their distinct approaches for taking advantage of the light environments in which they grow, influencing their absorption coefficient in the photosynthetically active radiation region. Thus, we analyzed the effects of the variance in crop structural and biochemical characteristics on the relationship between α_{par} vs. canopy [Chl] (Fig. 3).

The internal leaf structure of the crops studied is quite contrasting, with maize and rice exhibiting monocot leaves while soybean exhibits a dicot leaf. Monocots and dicots show different cell arrangements and chloroplast distributions within the leaves resulting in chlorophyll being more densely distributed within the palisade tissue of the soybean leaf, while more evenly distributed throughout the leaf thickness in both rice and maize. In addition, the three species evaluated exhibit two contrasting photosynthetic pathways that have evolved in combination with anatomical adaptations, such as the partitioning of photosynthetic activity between two morphologically distinct cell types known as the bundle sheath (BS) and the mesophyll (M). In C4 plants, such as maize, the BS and M cells surround the leaf veins in concentric circles, leading to a wreath-like appearance named the Kranz anatomy (Langdale, 2011). These anatomical differences, which are directly associated with the photosynthetic pathway, explain why soybean and rice (which is also a monocot like maize but has a C3 photosynthetic pathway like soybean) exhibit a more efficient absorption of PAR than maize for the same leaf [Chl] (Fig. 6). Note that in contrast to what was shown for

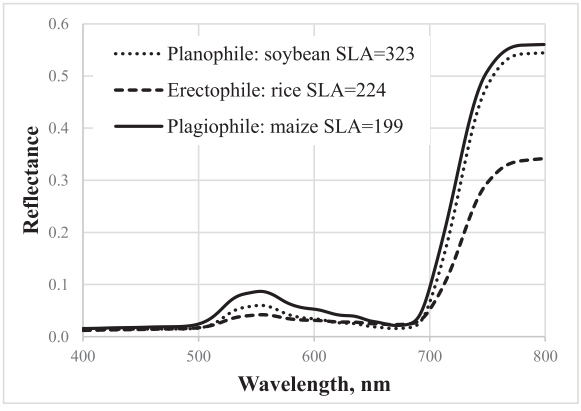

Fig. 8. Maize, soybean and rice canopy reflectance spectra simulated using PROSPECT-5 and SAIL models (Féret et al., 2017; Jacquemoud et al., 2009), for leaf [Chl] = 30 µg cm^{-2}, LAI = 3 m^2 m^{-2}, solar zenith angle = 30° and a default dry soil background (modified from Inoue et al., 2016). Specific leaf area (SLA) in cm^2 g^{-1} is defined as the ratio of total leaf area to total leaf dry mass.

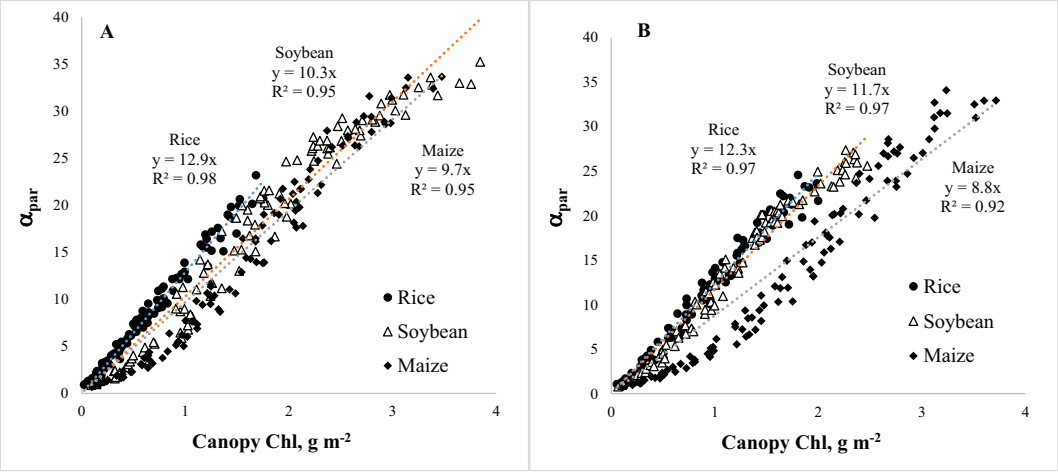

Fig. 9. Simulated relationships between α_{par} and canopy [Chl] for rice, soybean and maize using PROSPECT-D and SAIL models, under different input parameter variances. Case A: Full covariation of input parameters was allowed. Case B: Covariation of input parameters was restricted to match the variability observed along the growing season green LAI vs. canopy Chl relationship (Fig. 8). (For interpretation of the references to colour in this figure legend, the reader is referred to the web version of this article.)

canopy α_{par} (Fig. 5B), the relationship between leaf α_{par} vs. leaf [Chl] is essentially not-linear (Fig. 6). This is due to the strong saturation of leaf reflectance in the blue and the red spectral regions, which occurs even in slightly green leaves.

We also found that the relationship between green LAI and canopy [Chl] is species-specific (Fig. 7). The slope of this relationship - (leaf [Chl])$^{-1}$ - was highest in rice (3.21 m^2 g^{-1}) followed by soybean (2.27 m^2 g^{-1}) and then by maize (1.63 m^2 g^{-1}). This means that for the same canopy [Chl], which is a product of leaf [Chl] and green LAI, rice has a 2-fold higher green LAI than maize but a correspondingly smaller leaf [Chl], which is associated with a higher efficiency of light absorption by chlorophyll (Houborg et al., 2011).

3.2. Simulation analyses

To assess the effects of different LAD on canopy reflectance, we used simulations by a PROSAIL (Féret et al., 2017; Jacquemoud et al., 2009), with average values of specific leaf area (SLA, in cm^2 g^{-1}) for each species, performed by Inoue et al., (2016) for the same data sets (Fig. 8). These simulations show that reflectance in the PAR region is highly influenced by LAD, as it is the highest in maize followed by soybean and then by rice. While this may suggest that the effect of LAD on canopy reflectance is larger than that of leaf structure, it is important to underline that the distribution of chlorophyll within the leaves evaluated was only partially taken into account in these simulations through the differences in SLA. Thus, *the simulated spectra cannot explicitly explain the α_{par} vs. canopy [Chl] relationships observed* in soybean and rice for the same canopy [Chl] (Fig. 3). Therefore, the radiative transfer inside the canopies of these species is quite dissimilar.

It is important to note that the proper modeling of the radiative transfer in canopies with the unique green LAI vs. canopy [Chl] relationships (presented in Fig. 8) requires a specific combination of modeling parameters for each crop, particularly leaf [Chl] and green LAI, which, to the best of our knowledge, has not yet been considered. Furthermore, although a higher green LAI in soybean and especially in rice for the same canopy [Chl], increases the efficiency of light absorption, this factor was not considered in the simulation shown in Fig. 8 and thus *unrealistic combinations of input parameters, specifically green LAI and leaf [Chl], were used*. As has been recognized by other authors (Wocher et al., 2020; Yebra and Chuvieco, 2009), this shows that the use of look up tables can be a source of simulation of implausible spectra.

To address this issue, we evaluated two simulation approaches following different input parameter combinations. In the first approach (Case A; Fig. 9A), both green LAI and leaf [Chl] were allowed to co-vary from their minimum to their maximum values using the canopy architecture and specific leaf area of each crop (shown in Fig. 8) as has been reported for these crops (Inoue et al., 2016). This corresponds to a scenario in which there is a relevant temporal co-variation of both canopy structural and biochemical traits. In the second approach (Case B; Fig. 9B), the variability of both green LAI and leaf [Chl] was restricted in accord with empirically established green LAI vs. canopy [Chl] relationships (Fig. 7). *In this scenario the values of green LAI and leaf [Chl] for each crop correspond to those observed throughout the growing season.* In scenario A, slopes of α_{par} vs. canopy [Chl] relationships for rice, soybean and maize were 12.9, 10.3 and 9.7, respectively (Fig. 9A). The sensitivities of rice and soybean α_{par} to canopy [Chl] were far from similar as was found empirically (Fig. 3A). In Case B, as species-specific green LAI vs. canopy [Chl] relationships (and, thus, correspondence between green LAI and leaf [Chl] for each crop) were taken into account (Fig. 7), more reliable slopes of α_{par} vs. canopy [Chl] relationships were obtained illustrating the main features taken empirically (Fig. 3). In this case the slopes for rice, soybean and maize were 12.3, 11.7 and 8.8, respectively, and the difference in slopes between rice and soybean was about 5% (Fig. 9B).

4. Concluding remarks

The empirical and modeling results obtained in this study allowed us to explain some of the effects exerted by structural and biochemical plant traits on the absorption coefficient in the PAR region. On the one hand, the difference in the α_{par} vs. canopy [Chl] relationship observed between maize and rice may be explained mainly by differences in LAD and partly by the differences in leaf PAR absorption, which is more efficient in rice than in maize. On the other hand, the similarity in the α_{par} vs. canopy [Chl] relationship observed in rice and soybean may be explained by the cancellation of the significant differences in LAD (which is more efficient for light capture in rice) and in leaf [Chl] (which is more efficient for light capture in soybean) between these two crops. The difference in the α_{par} vs. canopy [Chl] relationship observed between soybean and maize may be explained by the significant differences in leaf α_{par} between these two crops. For the same canopy [Chl] the larger soybean leaf area is responsible for a more effective absorption of PAR by the soybean canopy.

The high sensitivity of α_{par} to the different canopy traits makes it particularly suitable for monitoring PAR absorption across different plant species, with different structures and biochemistries. Furthermore,

since α_{par} could be used to accurately retrieve canopy Chl, it constitutes a proxy of leaf Chl but only when canopy Chl content is closely related to leaf Chl content, which in the crops studied occurs during the reproductive and senescence stages. Under this circumstance, this provides an excellent opportunity for assessing remotely the photosynthetic status of vegetation, as leaf [Chl] relates with the maximum rate of rubisco activity. While the effects of other vegetation characteristics such as LAD and LAI were also initially evaluated through simulation, these, among several others (e.g., different pigment compositions), should be further studied to properly understand the influence of canopy and leaf structure and function on light absorption and photosynthesis rates.

The study also emphasized *the necessity of including information on within-leaf anatomical structure, together with the use of combinations of input parameters realistic for each species, in particular green LAI and leaf chlorophyll content, in integrated canopy reflectance models*. These are crucial for the successful application of generic spectral methods for assessing the photosynthetic status of plant species with different traits (e.g., C3, C4, monocot, dicot, erectophile, planophile, etc.), at multiple spatial scales ranging from individual canopies to entire geographic regions, and with a high temporal depth due to the long historical record of the Landsat sensor series.

Declaration of Competing Interest

Authors do not have any conflict of interest.

Acknowledgements

The support and use of facilities and equipment provided by the Center for Advanced Land Management Information Technologies (CALMIT), the School of Natural Resources, and the Carbon Sequestration Program, all at the University of Nebraska-Lincoln, are greatly appreciated. This research was partially supported by the Nebraska Agricultural Experiment Station with funding from the Hatch Act (Accession Number 1002649) through the USDA National Institute of Food and Agriculture. Funding for AmeriFlux data resources was provided by the U.S. Department of Energy's Office of Science. S. Skakun was supported by NASA grants 80NSSC18K0336 and 80NSSC18M0039. The authors are very thankful to three anonymous reviewers for their constructive suggestions that improved the manuscript quality.

References

Ciganda, V., Gitelson, A., Schepers, J., 2008. Vertical profile and temporal variation of chlorophyll in maize canopy: quantitative "crop vigor" indicator by means of reflectance-based techniques. Agron. J. 100, 1409–1417. https://doi.org/10.2134/agronj2007.0322.

Ciganda, V., Gitelson, A., Schepers, J., 2009. Non-destructive determination of maize leaf and canopy chlorophyll content. J. Plant Physiol. 166, 157–167.

Féret, J.-B., Gitelson, A., Noble, S., Jacquemoud, S., 2017. PROSPECT-D: towards modeling leaf optical properties through a complete lifecycle. Remote Sens. Environ. 193, 204–215.

Gitelson, A.A., Gamon, J.A., 2015. The need for a common basis for defining light-use efficiency: implications for productivity estimation. Remote Sens. Environ. 156, 196–201.

Gitelson, A.A., Viña, A., Ciganda, V., Rundquist, D.C., Arkebauer, T.J., 2005. Remote estimation of canopy chlorophyll content in crops. Geophys. Res. Lett. 32.

Gitelson, A.A., Viña, A., Verma, S.B., Rundquist, D.C., Arkebauer, T.J., Keydan, G., Leavitt, B., Ciganda, V., Burba, G.G., Suyker, A.E., 2006. Relationship between gross primary production and chlorophyll content in crops: implications for the synoptic monitoring of vegetation productivity. J. Geophys. Res. Atmos. 111.

Gitelson, A.A., Viña, A., Masek, J.G., Verma, S.B., Suyker, A.E., 2008. Synoptic monitoring of gross primary productivity of maize using Landsat data. IEEE Geosci. Remote Sens. Lett. 5, 133–137.

Gitelson, A.A., Peng, Y., Viña, A., Arkebauer, T., Schepers, J.S., 2016. Efficiency of chlorophyll in gross primary productivity: a proof of concept and application in crops. J. Plant Physiol. 201, 101–110.

Gitelson, A.A., Arkebauer, T.J., Suyker, A.E., 2018. Convergence of daily light use efficiency in irrigated and rainfed C3 and C4 crops. Remote Sens. Environ. 217, 30–37.

Gitelson, A., Viña, A., Solovchenko, A., Arkebauer, T., Inoue, Y., 2019. Derivation of canopy light absorption coefficient from reflectance spectra. Remote Sens. Environ. 231, 111276.

Goward, S.N., Huemmrich, K.F., 1992. Vegetation canopy PAR absorptance and the normalized difference vegetation index: an assessment using the SAIL model. Remote Sens. Environ. 39, 119–140.

Houborg, R., Anderson, M.C., Daughtry, C., Kustas, W., Rodell, M., 2011. Using leaf chlorophyll to parameterize light-use-efficiency within a thermal-based carbon, water and energy exchange model. Remote Sens. Environ. 115, 1694–1705.

Houborg, R., McCabe, M., Cescatti, A., Gao, F., Schull, M., Gitelson, A., 2015. Joint leaf chlorophyll content and leaf area index retrieval from Landsat data using a regularized model inversion system (REGFLEC). Remote Sens. Environ. 159, 203–221.

Inoue, Y., Guérif, M., Baret, F., Skidmore, A., Gitelson, A., Schlerf, M., Darvishzadeh, R., Olioso, A., 2016. Simple and robust methods for remote sensing of canopy chlorophyll content: a comparative analysis of hyperspectral data for different types of vegetation. Plant Cell Environ. 39, 2609–2623.

Jacquemoud, S., Verhoef, W., Baret, F., Bacour, C., Zarco-Tejada, P.J., Asner, G.P., François, C., Ustin, S.L., 2009. PROSPECT+ SAIL models: a review of use for vegetation characterization. Remote Sens. Environ. 113, S56–S66.

Langdale, J.A., 2011. C4 cycles: past, present, and future research on C4 photosynthesis. Plant Cell 23, 3879–3892.

Lichtenthaler, H., 1983. Differences in chlorophyll levels, fluorescence and photosynthetic activity of leaves from high-light and low-light seedlings. In: Metzner, H. (Ed.), Photosynthesis and plant productivity: joint Meeting of OECD and Studienzentrum Weikersheim, Ettlingen Castle (Germany), October 11-14, 1981. Wissenschaftliche Verlagsgesellschaft, Stuttgart.

Masek, J.G., Vermote, E.F., Saleous, N.E., Wolfe, R., Hall, F.G., Huemmrich, K.F., Gao, F., Kutler, J., Lim, T.-K., 2006. A Landsat surface reflectance dataset for North America, 1990-2000. IEEE Geosci. Remote Sens. Lett. 3, 68–72.

Nguy-Robertson, A., Gitelson, A., Peng, Y., Viña, A., Arkebauer, T., Rundquist, D., 2012. Green leaf area index estimation in maize and soybean: combining vegetation indices to achieve maximal sensitivity. Agron. J. 104, 1336–1347.

Peng, Y., Gitelson, A.A., Keydan, G., Rundquist, D.C., Moses, W., 2011. Remote estimation of gross primary production in maize and support for a new paradigm based on total crop chlorophyll content. Remote Sens. Environ. 115, 978–989.

Peng, Y., Nguy-Robertson, A., Arkebauer, T., Gitelson, A.A., 2017. Assessment of canopy chlorophyll content retrieval in maize and soybean: implications of hysteresis on the development of generic algorithms. Remote Sens. 9, 226.

Quebbeman, J., Ramirez, J., 2016. Optimal allocation of leaf-level nitrogen: implications for covariation of Vcmax and Jmax and photosynthetic downregulation. J. Geophys. Res. Biogeosci. 121, 2464–2475.

Rundquist, D., Perk, R., Leavitt, B., Keydan, G., Gitelson, A., 2004. Collecting spectral data over cropland vegetation using machine-positioning versus hand-positioning of the sensor. Comput. Electron. Agric. 43, 173–178.

Sage, R.F., Sultmanis, S., 2016. Why are there no C4 forests? J. Plant Physiol. 203, 55–68.

Schull, M., Anderson, M., Houborg, R., Gitelson, A.A., Kustas, W., 2015. Thermal-based modeling of coupled carbon, water, and energy fluxes using nominal light use efficiencies constrained by leaf chlorophyll observations. Biogeosciences 12, 1511–1523.

Verma, S.B., Dobermann, A., Cassman, K.G., Walters, D.T., Knops, J.M., Arkebauer, T.J., Suyker, A.E., Burba, G.G., Amos, B., Yang, H., 2005. Annual carbon dioxide exchange in irrigated and rainfed maize-based agroecosystems. Agric. For. Meteorol. 131, 77–96.

Viña, A., Gitelson, A.A., 2005. New developments in the remote estimation of the fraction of absorbed photosynthetically active radiation in crops. Geophys. Res. Lett. 32.

Viña, A., Gitelson, A.A., Nguy-Robertson, A.L., Peng, Y., 2011. Comparison of different vegetation indices for the remote assessment of green leaf area index of crops. Remote Sens. Environ. 115, 3468–3478.

Wocher, M., Berger, K., Danner, M., Mauser, W., Hank, T., 2020. RTM-based dynamic absorption integrals for the retrieval of biochemical vegetation traits. Int. J. Appl. Earth Obs. Geoinf. 93, 102219.

Wulder, M.A., Loveland, T.R., Roy, D.P., Crawford, C.J., Masek, J.G., Woodcock, C.E., Allen, R.G., Anderson, M.C., Belward, A.S., Cohen, W.B., 2019. Current status of Landsat program, science, and applications. Remote Sens. Environ. 225, 127–147.

Yebra, M., Chuvieco, E., 2009. Linking ecological information and radiative transfer models to estimate fuel moisture content in the Mediterranean region of Spain: solving the ill-posed inverse problem. Remote Sens. Environ. 113, 2403–2411.

Young, S.N., Sack, L., Sporck-Koehler, M.J., Lundgren, M.R., 2020. Why is C4 photosynthesis so rare in trees? J. Exp. Bot. 71, 4629–4636.